0026-895X/09/7505-1149–1159$20.00
MOLECULAR PHARMACOLOGY
Copyright © 2009 The American Society for Pharmacology and Experimental Therapeutics
Mol Pharmacol 75:1149–1159, 2009

Vol. 75, No. 5
54791/3468656
Printed in U.S.A.

Structural Determinants of Imidazoacridinones Facilitating Antitumor Activity Are Crucial for Substrate Recognition by ABCG2

Eran E. Bram, Yamit Adar, Nufar Mesika, Michal Sabisz, Andrzej Skladanowski, and Yehuda G. Assaraf

The Fred Wyszkowski Cancer Research Laboratory, Department of Biology, Technion-Israel Institute of Technology, Haifa, Israel (E.E.B., Y.A., N.M., Y.G.A.); and Laboratory of Cellular and Molecular Pharmacology, Department of Pharmaceutical Technology and Biochemistry, Gdansk University of Technology, Gdansk, Poland (M.S., A.S.)

Received January 15, 2009; accepted February 25, 2009

ABSTRACT

Symadex is the lead acridine compound of a novel class of imidazoacridinones (IAs) currently undergoing phase II clinical trials for the treatment of various cancers. Recently, we have shown that Symadex is extruded by ABCG2-overexpressing lung cancer A549/K1.5 cells, thereby resulting in a marked resistance to certain IAs. To identify the IA residues essential for substrate recognition by ABCG2, we here explored the ability of ABCG2 to extrude and confer resistance to a series of 23 IAs differing at defined residue(s) surrounding their common 10-azaanthracene structure. Taking advantage of the inherent fluorescent properties of IAs, ABCG2-dependent efflux and drug resistance were determined in A549/K1.5 cells using flow cytometry in the presence or absence of fumitremorgin C, a specific ABCG2 transport inhibitor. We find that a hydroxyl group at one of the R1, R2, or R3 positions in the proximal IA ring was essential for ABCG2-mediated efflux and consequent IA resistance. Moreover, elongation of the common distal aliphatic side chain attenuated ABCG2-dependent efflux, thereby resulting in the retention of parental cell sensitivity. Hence, the current study offers novel molecular insight into the structural determinants that facilitate ABCG2-mediated drug efflux and consequent drug resistance using a unique platform of fluorescent IAs. Moreover, these results establish that the IA determinants mediating cytotoxicity are precisely those that facilitate ABCG2-dependent drug efflux and IA resistance. The possible clinical implications for the future design of novel acridines that overcome ABCG2-dependent multidrug resistance are discussed.

The frequent emergence of anticancer drug resistance phenomena continues to be a major impediment toward curative chemotherapy of various human malignancies (Modok et al., 2006). In this respect, multidrug resistance (MDR) is perhaps the most extensively studied major mechanism of chemoresistance (Sarkadi et al., 2006; Sharom, 2008). MDR is mediated by members of the ATP-binding cassette superfamily of transporters, including ABCB1 (P-glycoprotein), ABCC1 (MRP1), and ABCG2 (breast cancer resistance protein) (Borst and Elferink, 2002; Doyle and Ross, 2003; Deeley et al., 2006; Polgar et al., 2008). These ATP-driven efflux pumps, which recognize a plethora of hydrophobic, hydrophilic and amphiphilic compounds, extrude out of malignant cells structurally distinct endo- and xenobiotics, many of which are key antitumor agents, thereby resulting in a wide spectrum of MDR.

Recent studies have shown that increased expression of ABCG2 before chemotherapy may underlie inherent drug resistance of tumors, including acute myeloid leukemia (AML) treated with established ABCG2 substrates such as mitoxantrone, topotecan, and doxorubicin (Ross et al., 2000). In this respect, high ABCG2 levels were detected in approximately one third of the patients in an experiment that used reverse transcriptase polymerase chain reaction to determine ABCG2 transcript levels in AML blast cells (Ross et al., 2000). Subsequent studies observed a tight correlation between ABCG2 mRNA levels and the viability of acute leukemia blast cells in the presence of the cyclin-dependent kinase inhibitor flavopiridol (Nakanishi et al., 2003). Hence, ABCG2-dependent MDR may lead to incomplete eradication of leukemic cells, thereby resulting in clonal expansion and

Article, publication date, and citation information can be found at http://molpharm.aspetjournals.org.
doi:10.1124/mol.109.054791.

ABBREVIATIONS: AML, acute myeloid leukemia; IA, imidazoacridinone; TA, triazoloacridinone; MTT, 3-(4,5-dimethylthiazol-2-yl)-2,5-diphenyltetrazolium bromide; FTC, fumitremorgin C; ABC, ATP-binding cassette; PhA, pheophorbide ; PBS, phosphate-buffered saline; TMR, tetramethylrosamine; RF, resistance-fold; AF, accumulation-fold; ClogP, calculated log P; MDR, multidrug resistance.

relapse of a chemoresistant disease. This is in accord with recent observations that ABCG2 mRNA levels were significantly increased in relapsed AML (Steinbach et al., 2002; van den Heuvel-Eibrink et al., 2002). Hence, the development of novel modalities that overcome ABCG2-dependent MDR phenomena in various human cancers is one of the major goals of current preclinical cancer therapeutics and an ongoing pursuit in the field of rational drug design.

Symadex (formerly C-1311) is the lead compound in clinical development of a novel series of acridine cytotoxic agents known as imidazoacridinones (IAs) (Cholody et al., 1990a,b; Kusnierczyk et al., 1994; Burger et al., 1996; Dziegielewski et al., 2002; Hyzy et al., 2005; Bram et al., 2007). In preclinical studies, Symadex has shown cytotoxic activity apparently via several mechanisms of action. Whereas Hyzy et al. (2005) showed that Symadex cytotoxicity is exerted through a prolonged G_2 arrest followed by mitotic catastrophe, recent reports reveal that Symadex is a potent and selective FLT3 receptor tyrosine kinase inhibitor (Stam et al., 2004; Goodman et al., 2008). Specifically, Symadex is currently undergoing phase II clinical trials as a novel anticancer drug, including colorectal cancer (Alami et al., 2007). Moreover, Symadex is undergoing preclinical testing for the possible treatment of non-neoplastic disorders, such as autoimmune diseases, as well as multiple sclerosis and rheumatoid arthritis, where early preclinical data have shown promising pharmacological activity.

IAs share common structural features with various chemotherapeutic drugs and naturally occurring bioactive compounds, thereby establishing them as bona fide model drugs. In this respect, we have recently shown that Symadex is efficiently extruded by ABCG2-overexpressing A549/K1.5 lung cancer cells (Cholody et al., 1990b; Bram et al., 2007). Here we explored the possibility of establishing a practical approach for the discovery of drug determinants facilitating ABCG2-dependent MDR in human cancers, using this novel group of IAs. Toward this end and taking advantage of the intense fluorescent properties of a large series of structurally related IAs, we here provide the first evidence for the absolute requirement of the presence of a hydroxyl group at the proximal external ring of the imidazoacridinone structure of IAs in order for ABCG2 to recognize and extrude these antitumor agents. We further demonstrate that lung cancer cells overexpressing ABCG2 display a marked hypersensitivity to certain IAs that lack a hydroxyl group. This latter finding holds promise for the future synthesis of novel IAs that not only evade the ABCG2-dependent MDR phenotype, but also render MDR cells hypersensitive to these antitumor agents. Hence, these novel findings bear important clinical implications for the overcoming of ABCG2-dependent MDR.

Materials and Methods

Drugs and Chemicals. All IAs and triazoloacridinones (TAs) were synthesized in the Department of Pharmaceutical Technology and Biochemistry by Drs. M. Cholody, B. Horowska, and M. Konieczny. Compounds were dissolved in 0.2% lactic acid and stored at −24°C until use. 3-(4,5-Dimethylthiazol-2-yl)-2,5-diphenyltetrazolium bromide (MTT) and tetramethylrosamine were obtained from Sigma Chemical Co. (St. Louis, MO). Fumitremorgin C (FTC) and pheophorbide (PhA) were kindly provided by Dr. S. E. Bates (National Cancer Institute, Bethesda, MD). G-418 hydrochloride was purchased from Calbiochem-Novabiochem (San Diego, CA).

Tissue Culture. Human non–small-cell lung cancer A549 cells and T-cell leukemia CCRF-CEM cells were grown under monolayer conditions or up to a maximal density of 10^6 cells/ml (for CCRF-CEM cells) in RPMI 1640 medium (Invitrogen, Carlsbad, CA) supplemented with 10% fetal calf serum, 2 mM glutamine, 100 μg/ml penicillin, and 100 μg/ml streptomycin (Biological Industries, Beth-Haemek, Israel) in a humid atmosphere of 5% CO_2. Drug-resistant A549/K1.5 cells with ABCG2 overexpression were maintained under a continuous drug selection with 1.5 μM C-1305 (Bram et al., 2007). For cytotoxicity and accumulation experiments, cells were grown in drug-free medium for at least 1 week before the experiments. Human embryonic kidney (HEK) 293 cells and their stable transfectants overexpressing the Arg482, Gly482, and Thr482 ABCG2 (Bram et al., 2006) were grown in RPMI 1640 medium supplemented with 2 mg/ml G-418.

Cytotoxicity and Growth Inhibition Assays. The cytotoxic activity of the various IAs and TAs was determined using the colorimetric MTT assay (Poindessous et al., 2003). Exponentially growing cells were seeded at 5×10^3 cells/well in 24-well plates (2 ml of medium/well). After an overnight incubation, cells were exposed to different drug concentrations for 120 h. Cellular viability was determined by adding the tetrazolium salt MTT for 4 h at 37°C, followed by solubilization of the intracellular precipitated formazan in 1 ml of dimethyl sulfoxide, and absorbance was determined by a microplate reader (ASYS Hitech, GmbH, Austria). Drug concentrations required to inhibit cell growth by 50% (IC_{50}) compared with untreated controls were determined from the curves of survival versus drug concentrations using the SlideWrite software (Advanced Graphics Software, Inc., Encinitas, CA). Resistance factors (RF) were calculated by dividing the IC_{50} value of drug resistant cells by that of the parental counterpart. Values presented are means of at least three independent experiments, each performed in duplicate.

Flow Cytometric Assay of Cellular Accumulation. One milliliter aliquots of A549/K1.5 or CCRF-CEM cell suspensions (1×10^6 cells/ml) in growth medium containing 20 mM HEPES at pH 7.3 were distributed into 1.5-ml polypropylene Eppendorf test tubes. Then, IAs were added at increasing concentrations of 0.1 to 300 μM, in the presence or absence of the specific ABCG2 efflux inhibitor FTC (5 μM) (Rabindran et al., 2000) and allowed to incubate for 1 h at 37°C. Alternatively, in the time-course experiments, IAs at a constant concentration of 10 μM were added to a CCRF-CEM cell suspension incubated at 37°C and 1-ml aliquots were removed at various time points up to 1 h. After incubation, the test tubes were transferred to ice and centrifuged at 4°C. Cells were then washed twice and resuspended in ice-cold PBS containing 1% fetal calf serum and kept in the dark at 4°C until analysis. IA and tetramethylrosamine (TMR) accumulation in parental HEK293 and their stable HEK/Arg482ABCG2, Gly482, and Thr482 transfectants (Robey et al., 2003) were carried out as described above with the slight amendment of using a constant IA concentration of 1 μM ± FTC (5 μM) or a 0.1 μM TMR concentration. Reciprocal competitive accumulation assay using PhA and IAs were carried out as described above. Alternatively, IAs C-1309 and C-1310 as well as PhA were used as the fluorescent accumulating probe at a constant concentration of 25 nM, whereas their reciprocal use as potential competitive ABCG2 inhibitors was at a molar excess of up to 40- and 1000-fold. Cellular fluorescence was determined using a FACSCalibur (BD Bioscience, San Jose, CA) flow cytometer. FL1-H excitation of IAs was at 488 nm, and emission was collected at 525 nm; FL2-H excitation of TMR was at 550 nm and emission was collected at 574 nm; the FL-4 excitation of PhA was at 630 nm and emission was collected at 660 nm. Flow cytometric results are presented either as a representative experiment or as mean ± S.D. of at least three independent experiments.

Immunofluorescence Microscopy of Plasma Membrane Targeting of ABCG2 and Nuclear Accumulation of IAs. Cells (1×10^4/well) were seeded in 24-well plates (1 ml of medium/well) and incubated for 2 days, after which some wells were supplemented

with 10 μM IA-containing medium ± 5 μM FTC. After 1-h incubation at 37°C, cells were washed twice with ice-cold PBS containing 0.1% BSA and blocked for 10 min at 4°C with PBS containing 5% BSA. Cells were then washed once with ice-cold PBS containing 0.1% BSA and incubated for 30 min at 4°C with a phycoerythrin-conjugated, affinity-purified 5D3 mouse anti-human ABCG2 monoclonal antibody (1:100; eBioscience, San Diego, CA). The level of unspecific fluorescence was determined using cells that were incubated only with a secondary phycoerythrin-conjugated goat anti-mouse IgG (1:200; Jackson Immunoresearch Labs, West Grove, PA). Cells were then washed twice and subjected to fluorescence microscopy using a DMIRE2 fluorescence microscope equipped with a DC300FX camera (Leica Microsystems, Wetzlar, Germany).

Quantitative Evaluation of ABCG2 Interaction with Various IAs. The extent of ABCG2-dependent resistance was expressed using the resistance-fold (RF) parameter representing the ratio between the IC_{50} values of the drug-resistant cells and drug-sensitive parental cells. Likewise, ABCG2-dependent differential accumulation of IAs in ABCG2-overexpressing A549/K1.5 cells was compared using the ratio of IA accumulation in the presence or absence of FTC. This was termed the FTC-dependent accumulation-fold (AF) and was determined for each IA at a constant IA concentration of 10 μM. The accumulation of IAs at this constant concentration was found to be both readily detectable by flow cytometry and at nonsaturating levels and within the linear concentration–dependent range of drug accumulation for all IAs tested.

To assess the relative contribution of the various structural determinants of IAs to their ability to be extruded and induced drug resistance via ABCG2, we divided IAs into subgroups. Comparison was carried out within these subgroups; each subgroup contained structurally identical IAs that differed solely at a single structural determinant. Within each subgroup, the effect of the specific structural change on ABCG2-IA interaction was evaluated using a combined parameter termed the relative ABCG2-IA interaction. This parameter was calculated by averaging the relative percent RF and AF values for each IA within the subgroup, thereby generating a combined mean ± S.E. value.

Statistical Analyses. We used a nonpaired Student's t test to examine the significance of the difference between two populations for a certain variable and a one-tailed Z test to examine the significance of the difference between a population and a specific sample. A difference was considered significant if the P value obtained was <0.05. To explore the possible mathematical relationship between two paired data sets of two variables, a linear curve fit analysis was applied (Excel 2007; Microsoft Corp., Redmond, WA). R^2 values are presented, and the significance of correlation (P value) was assessed using a student's t test.

Calculations of Log *P* Values. The lipophilicity parameter log P was calculated for the various IAs using the SPARC (Predictive Modeling System) online server at the U.S. Environmental Protection Agency (Research Triangle Park, NC) as described previously (Bram et al., 2007).

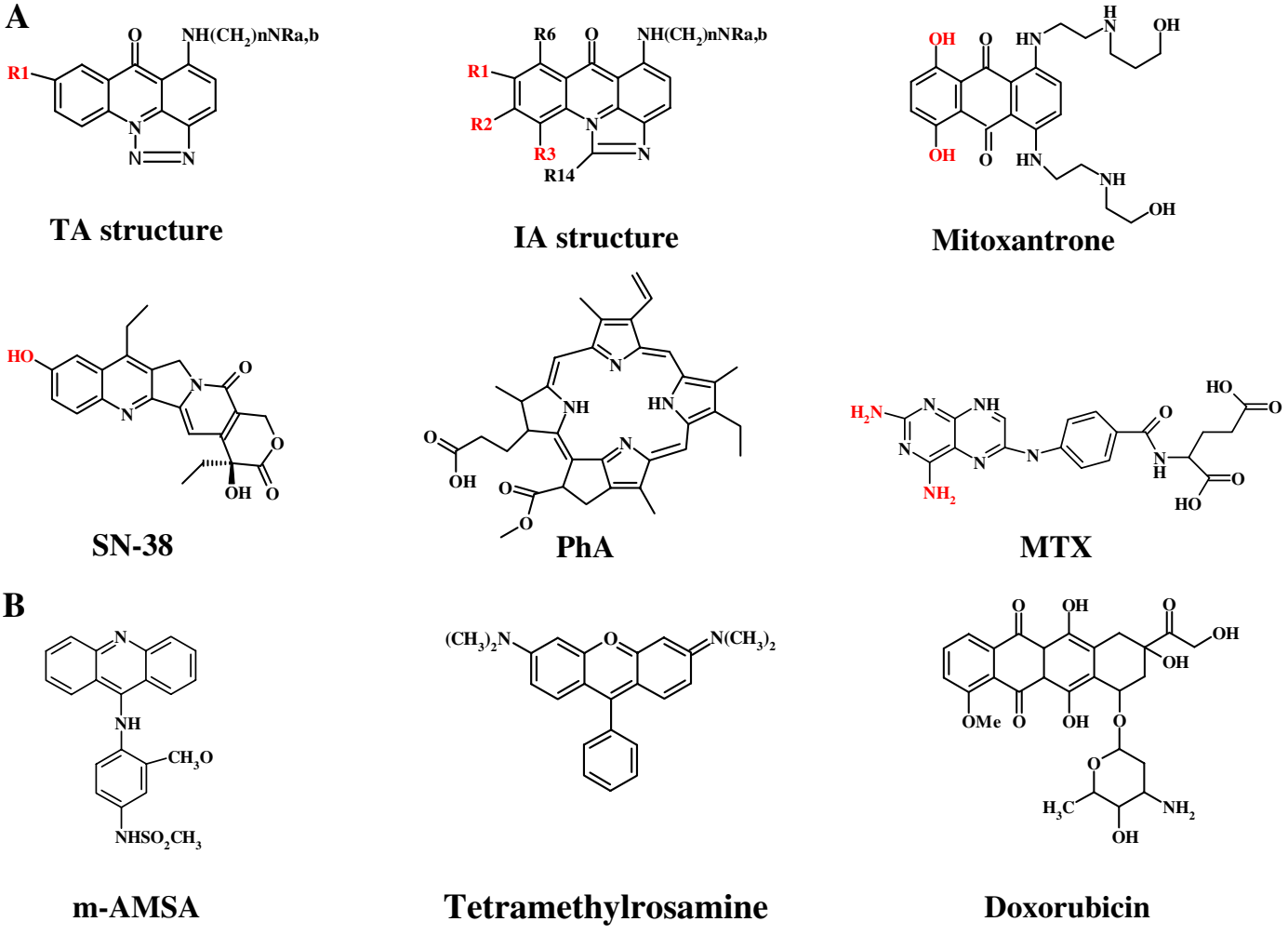

Fig. 1. Structural formulas of IAs and various polycyclic chemotherapeutic agents. ABCG2 substrates containing a putative hydrogen bond donor (red) necessary for interaction with ABCG2 (A) as well as structurally similar polycyclic drugs known as non-ABCG2 substrates that lack the positional hydrogen bond donor group (B).

Results

Differential Resistance of ABCG2-Overexpressing A549/K1.5 Cells to Certain IAs. We have recently shown that ABCG2 overexpression is the molecular mechanism underlying resistance of A549/K1.5 cells to the IA Symadex (C-1311) (Bram et al., 2007). To assess the levels of drug resistance of A549/K1.5 cells to a series of 23 IA analogs that were different at seven defined residues surrounding their common imidazoacridone structure (Fig. 1), MTT-based cytotoxicity assays were used (Table 1). A549/K1.5 cells displayed a differential resistance toward certain IA derivatives, thereby subdividing them into two distinct groups (P = 0.0007) termed group A and B, hence representing drugs to which ABCG2 overexpression confers resistance or fails to do so, respectively (Table 1 and Fig. 2). Specifically, A549/K1.5 cells exhibited a prominent resistance to C-1311 as well as to nine other IAs, including C-1309, C-1336, C-1310, C-1584, C1371, C-1335, C-1419, C-1492, and C-1633 (group A), with up to 61-fold resistance to C-1309. In contrast, A549/K1.5 cells retained near parental cell sensitivity to the 13 remaining IAs (group B), with the exception of C-1330 and C-1266, to which A549/K1.5 cells displayed 2.2- and 5.0-fold hypersensitivity, respectively (Table 1 and Fig. 2). Thus, these results establish that ABCG2 recognizes certain IA derivatives but fails to do so with other IAs.

Drug Resistance Correlates with Reduced Cellular Accumulation of IAs. The results given in Table 1 and Fig. 2 suggest that overexpression of ABCG2 is the molecular mechanism underlying resistance of A549/K1.5 cells to group A IAs. To corroborate this finding, we further explored the ability of ABCG2 to extrude IAs from A549/K1.5 cells using the intrinsic fluorescent properties of IAs in a flow cytometric assay. A549/K1.5 cells displayed a complete exclusion of group A IAs, up to high micromolar drug concentrations (see a representative IA of both groups A and B, Fig. 3, A and B). Furthermore, addition of the specific ABCG2 transport inhibitor FTC resulted in a concentration-dependent restoration of drug accumulation of group A IAs (Fig. 3A). In contrast, A549/K1.5 cells accumulated group B IAs in a concentration-dependent manner regardless of the presence or absence of FTC (Fig. 3B). To quantify the ABCG2-dependent component of IA accumulation in A549/K1.5 cells, we used the parameter of FTC-dependent accumulation fold (AF; see *Materials and Methods*) for each IA, at a constant IA concentration of 10 μM. This quantitative analysis revealed the same IA cluster distribution observed in the above cytotoxicity assay (P = 0.0002; compare Fig. 3C and Fig. 2). Accordingly, group A IAs exhibited high AF values ranging from 9.4 to 47.1, hence representing the FTC-reversible, ABCG2-dependent restoration of IA drug accumulation. In contrast, group B IAs consisting of non-ABCG2 substrates retained AF values close to 1.0. Moreover, when plotting the RF values versus the AF values, a distinct separation was observed between these clusters, with an integrated average cluster difference of 16.8-fold (Fig. 3D). Hence, this two-dimensional functional representation defines and subdivides these IA compounds into two distinct groups regarding ABCG2-mediated drug efflux and consequent drug resistance.

Nuclear and Perinuclear Localization Is a Hallmark of Intracellular Accumulation of IAs. C-1311 and other acridine-based compounds display nuclear and perinuclear accumulation and exert their cytotoxic activity via direct interaction with DNA as well as with DNA-modifying enzymes including topoisomerase I or II (Topcu, 2001; Belmont et al., 2007). To exclude the possibility that differential subcellular accumulation of IAs is the basis of the observed difference in cytotoxicity and cellular fluorescence, A549/K1.5 cells were incubated with 10 μM concentrations of selected IAs from groups A and B in the presence or absence of FTC and subjected to fluorescence microscopy. Consistent with the flow cytometric results (Fig. 3, A–C), group A compounds C-1311 and C-1310 showed no apparent intracellular accumulation in A549/K1.5 cells that overexpress functional ABCG2 at the plasma membrane (Fig. 4, A

TABLE 1
Summary of growth inhibition studies on parental A549 and ABCG2 expressing A549/K1.5 cells upon 120-h exposure to the various IAs
IC_{50} was evaluated using the MTT assay.

Drug	IC_{50}		RF
	A549	A549/K1.5	
	μM		
Group A			
C-1309	0.05 ± 0.007	3.22 ± 0.180	60.80
C-1336	0.058 ± 0.12	2.41.1 ± 1.1	41.55
C-1310	0.06 ± 0.008	1.22 ± 0.070	20.30
C-1584	0.01 ± 0.002	0.25 ± 0.010	19.20
C-1371	0.04 ± 0.006	0.70 ± 0.030	17.90
C-1335	0.09 ± 0.004	1.00 ± 0.250	11.10
C-1419	2.92 ± 0.420	31.26 ± 2.550	10.70
C-1492	1.69 ± 0.120	17.17 ± 1.950	10.10
C-1311	0.27 ± 0.012	2.34 ± 0.050	8.70
C-1633	2.26 ± 0.330	9.83 ± 1.440	4.35
C-1315	1.69 ± 0.260	3.46 ± 0.160	2.05
C-1558	1.48 ± 0.250	2.51 ± 0.170	1.70
C-1554	2.02 ± 0.330	3.07 ± 0.800	1.51
C-1213	12.28 ± 2.500	18.27 ± 2.400	1.49
C-2018	1.54 ± 0.310	2.13 ± 0.620	1.38
C-1212	1.89 ± 0.420	1.93 ± 0.840	1.02
C-1375	1.30 ± 0.060	1.25 ± 0.110	0.96
Group B			
C-1415	2.70 ± 0.210	2.38 ± 0.120	0.88
C-1503	3.50 ± 0.640	3.09 ± 0.740	0.88
C-1379	1.07 ± 0.030	0.68 ± 0.060	0.63
C-1176	2.35 ± 0.750	1.21 ± 0.650	0.51
C-1330	2.16 ± 0.270	0.97 ± 0.080	0.45
C-1266	2.81 ± 0.270	0.56 ± 0.002	0.20

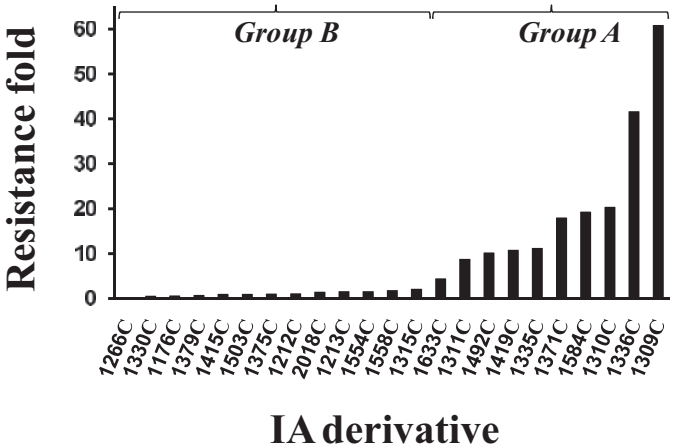

Fig. 2. RF values of ABCG2 overexpressing A549/K1.5 cells to 23 IAs compared with parental A549 cells. Parental A549 and ABCG2-overexpressing A549/K1.5 cells were exposed for 96 h to increasing concentrations of the various 23 IAs followed by IC_{50} determination using a colorimetric MTT assay. Results depicted represent RF determined by dividing the IC_{50} values obtained with ABCG2-overexpressing A549/K1.5 by that of parental A549 cells.

and C, red fluorescence). However, a marked restoration of nuclear accumulation of these ABCG2 substrates occurred upon inhibition of ABCG2 efflux activity by FTC (Fig. 4, B and D, green fluorescence). In contrast, the non-ABCG2 substrate C-1213 from group B displayed comparable and significant nuclear accumulation regardless of ABCG2 inhibition by FTC (Fig. 4, E and F).

Group A and B IAs Accumulate in a Comparable Concentration- and Time-Dependent Manner in ABCG2-null CCRF-CEM Leukemia Cells. Intracellular drug accumulation is thought to represent a net drug influx superseding all cellular efflux mechanisms, including those mediated by ABC transporters. Therefore, to rule out the possibility that the observed difference in intracellular accumulation of

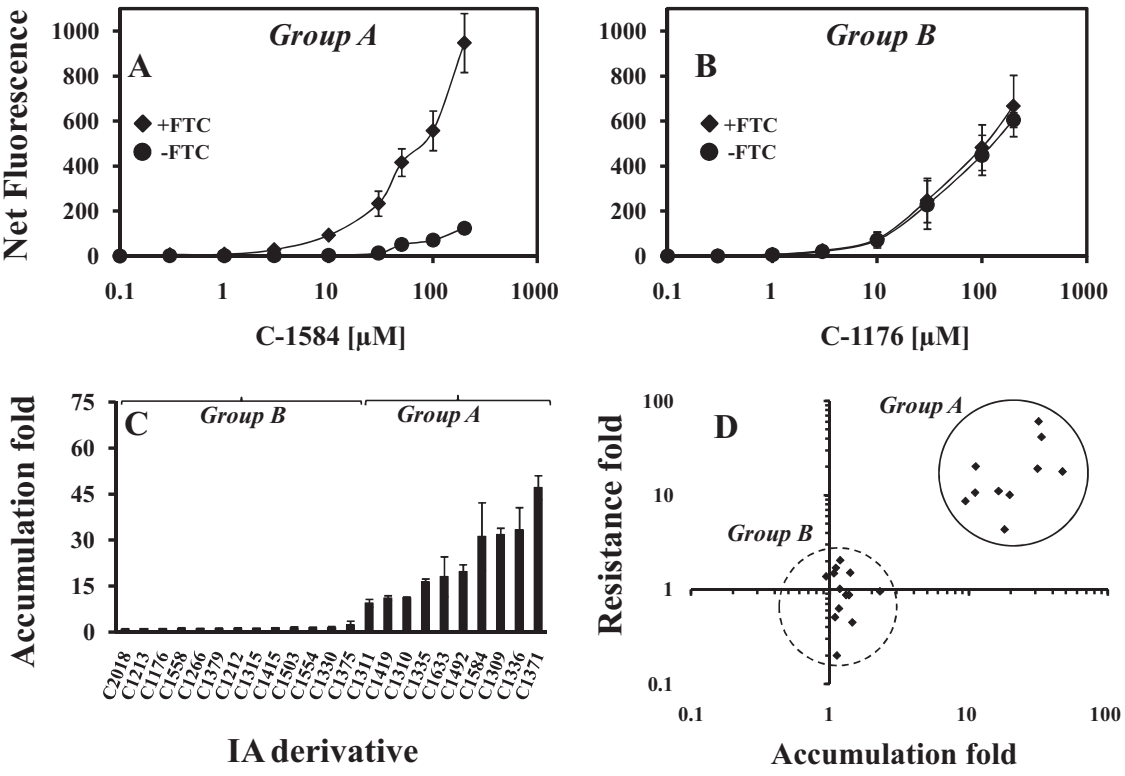

Fig. 3. Comparative exclusion levels of IAs from A549/K1.5 cells in the presence or absence of the ABCG2 transport inhibitor fumitremorgin C. A549/K1.5 cells were suspended in RPMI 1640 medium buffered with 20 mM HEPES, pH 7.3, containing increasing concentrations of the various IAs ranging from 0.01 to 200 μM and incubated for 1 h at 37°C in both the presence and the absence of 5 μM FTC. Mean net fluorescence at the various concentrations of group A representative IA C-1584 (A) or group B representative IA C-1176 (B) from at least three independent experiments is shown ± S.D. (C). Quantitative comparison of FTC-inducible IA AF at a constant IA concentration of 10 μM. Results depicted are means ± S.D obtained from three or more independent experiments (D). Clustering of the various IAs on a dot plot of RF versus AF.

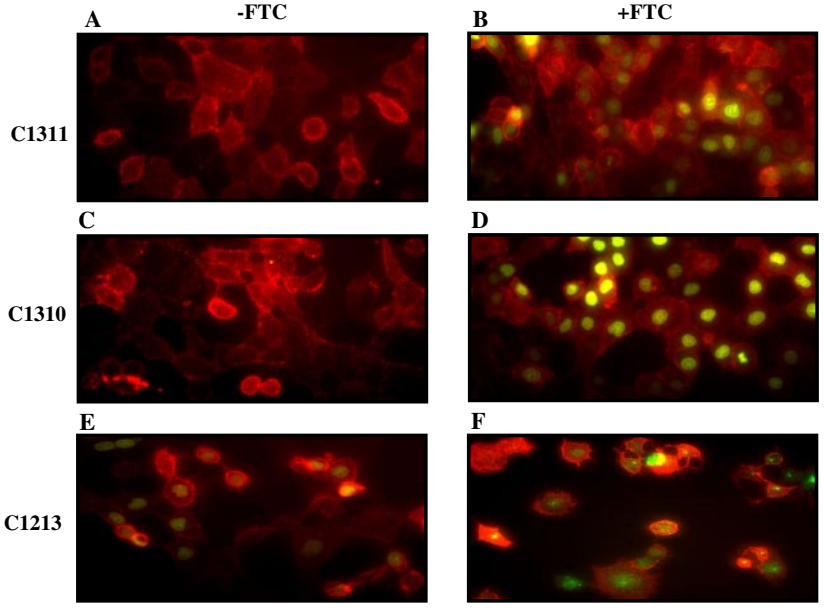

Fig. 4. Functionality of the overexpressed ABCG2 in A549/K1.5 cells as revealed by surface 5D3 antibody immunofluorescence and fluorescent nuclear accumulation of representative group A and B IAs. A549/K1.5 cells growing in monolayers were incubated for 1 h at 37°C with 10 μM concentrations of selected group A IAs: C-1311 (A and B), C-1310 (C and D) or the group B IA C-1213 (E and F), in the presence (right column) or absence (left column) of 5 μM FTC. Live cells were then subjected to immunolabeling using a phycoerythrin-conjugated 5D3 antibody directed to an extracellular ABCG2 epitope and examined by immunofluorescence microscopy.

IAs and subsequent cytotoxicity represented differential kinetics of IA uptake, we performed experiments aimed at comparing the time course and concentration-dependence of drug accumulation of group A and B IAs in CCRF-CEM human leukemia cells lacking ABCG2 expression (Turner et al., 2006). Comparable uptake rates and steady-state levels were observed for IAs from groups A and B as well as for PhA, a well established ABCG2 substrate (Fig. 5A). We next assessed the concentration-dependence of IA accumulation in these ABCG2-null leukemia cells (Fig. 5B). All IAs studied, including PhA, displayed a comparable concentration-dependent and saturable accumulation up to a concentration of 300 μM, thereby suggesting similar accumulation kinetics (Fig. 5B). Hence, these results support the conclusion that an ABCG2-dependent, differential IA efflux capacity is the mechanism underlying decreased intracellular accumulation of group A IAs and not distinct drug accumulation kinetics.

A Hydroxyl Group at One of the R1, R2 or R3 Positions Surrounding the Outer Ring of the IA Common Structure Mediates ABCG2-Dependent Drug Efflux and Resistance. Two-dimensional structural alignment of the various IAs revealed a distinct difference between the two IA groups (Table 2). Group A of ABCG2 substrates contains a hydroxyl group at position R1 of the common IA structure, except C-1419 and C-1633, which possess a hydroxyl group at positions R2 and R3, respectively (Table 2). All hydroxyl positions, including R1, R2, and R3, are located around the outer proximal IA ring. In contrast, most of the IAs from group B of non-ABCG2 substrates lack a hydroxyl group at the R1, R2, and R3 positions and contain various nonpolar substitutions at these positions. Nonetheless, both C-1315 and C-2018 of group B, which possess a hydroxyl group at position R1, failed to display any significant interaction with ABCG2 (Table 2).

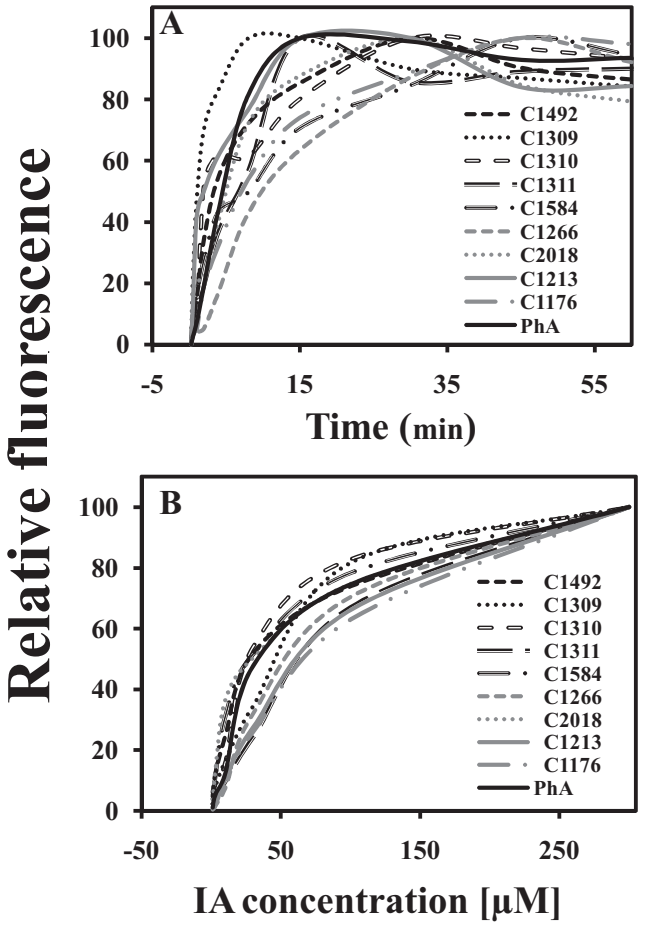

Fig. 5. Time course and concentration-dependent accumulation of group A and B IAs in ABCG2 lacking human leukemia CCRF-CEM cells. Cells were suspended in RPMI 1640 medium buffered with 20 mM HEPES, pH 7.3, and incubated with 10 μM concentrations of representative group A and B IAs for various times up to 1 h (A). Another portion of the cells was incubated for 1 h in various concentrations of the selected IAs (B). Time course and dose-dependent IA accumulation was then analyzed using flow cytometry. Results depicted are means obtained from three independent experiments (± S.D. ≤ 21%).

Elongation of the IA Side Chain Abolishes ABCG2-Mediated IA Efflux and Drug Resistance. C-1315 and C-2018 were found to be non-ABCG2 substrates despite the fact that they harbor a hydroxyl group at position R1. Close examination of the structure of these compounds reveals that both compounds possess the longest IA side chain (Table 2). We therefore hypothesized that this exception to the general requirement of a hydroxyl group at the R1, R2, or R3 positions reflected a negative impact that the length of the IA side chain (i.e., tail) had on the ability of ABCG2 to recognize and expel C-1315 and C-2018. The length of the IA tail varies at two positions: the alkane length (n) and the distal branched $R_{a,b}$ chain (Table 2). C-1315 possesses a C = 10 tail composed of an alkane group of C = 2 as well as an additional large branched $R_{a,b}$ chain of C = 8 (Table 2). Furthermore, C-2018 has a C = 13 tail consisting mainly of a long (C = 9) alkane group and a shorter branched $R_{a,b}$ chain of C = 4

TABLE 2
Two-dimensional structural comparison of the various IAs
IA common structure is presented.

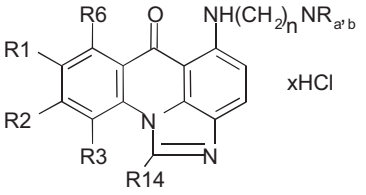

	R1	R2	R3	R6	R14	$R_{a,b}$	n
Group A							
C-1584	OH	H	H	H	H	Me	2
C-1311	OH	H	H	H	H	Et	2
C-1371	OH	H	H	H	H	Me	3
C-1335	OH	H	H	H	H	Et	3
C-1309	OH	H	H	H	Me	Me	2
C-1310	OH	H	H	H	Me	Et	2
C-1336	OH	H	H	H	Me	Et	3
C-1492	OH	H	H	H	H	Me	5
C-1419	H	OH	H	H	H	Et	2
C-1633	H	H	OH	H	H	Et	2
Group B							
C-1176	H	H	H	H	H	Me	2
C-1415	H	H	H	H	H	Et	2
C-1212	H	H	H	H	H	Me	3
C-1213	H	H	H	H	Me	Me	2
C-1266	H	H	H	H	H	Me	5
C-1503	H	H	OMe	OMe	H	Et	2
C-1554	Me	H	H	H	H	Et	2
C-1330	OMe	H	H	H	H	Et	2
C-1558	*t*-Butyl	H	H	H	H	Et	2
C-1375	OMe	H	H	H	Me	Me	3
C-1379	OMe	H	H	H	Me	Et	3
C-1315	OH	H	H	H	Me	Bu	2
C-2018	OH	H	H	H	H	Et	9

(Table 2). To test our hypothesis, the effect of IA's tail length on ABCG2-dependent transport of IA was evaluated within several sets of IAs differing only by the length of their branched side chain [i.e., $R_{a,b}$ or the alkane length (n)]. We determined the relative impact of IA's tail length on ABCG2-dependent transport of IA using an integrated parameter termed the relative ABCG2-IA interaction value (see *Materials and Methods*); the latter is composed of the two established parameters described under *Materials and Methods*: 1) ABCG2-mediated drug efflux (AF) and 2) drug resistance levels (RF). The relative ABCG2-IA interaction parameter reflects the averages of relative (%) RF and AF values for each IA within the compared subset. Indeed, with all IA compounds studied, ABCG2 interaction with these compounds revealed an inverse correlation with IA branched tail group $R_{a,b}$ length (Fig. 6A). Elongation of $R_{a,b}$ resulted in a significant decrease in the interaction of ABCG2 with IAs ($P < 0.03$; Fig. 6A). It is noteworthy that elongation of the alkane tail (n) seemed to have a lesser effect on ABCG2-mediated efflux and drug resistance. No significant decrease in ABCG2-IA interaction was observed for the IA pairs C-1584/C-1371 and C-1311/C-1335 ($P = 0.51$ and 0.11, respectively; Fig. 6B), both shifting from $n = 2$ to $n = 3$ alkane tail length (Table 2). However, a further marked increase in tail length (n) in C-1492 ($n = 5$) or C-2018 ($n = 9$) (Table 2) resulted in a statistically significant decrease in the ABCG2-IA interaction values ($P = 0.013$ and 0.004, respectively; Fig. 6B). Shifting the position of the ABCG2 interacting hydroxyl group from R1 to R2, or from R1 to R3, revealed a marked decrease in IA cytotoxicity (Table 1) but did not significantly affect ABCG2-IA interaction ($P > 0.31$; Fig. 6C).

The Relative ABCG2-IA Interaction Values Correlate with IAs Cytotoxicity but Not with IA ClogP Values. When plotting the relative ABCG2-IA interaction values of the various IAs with short tails versus their cytotoxicity values (IC_{50}; Table 1), an inverse correlation was observed (Fig. 7A). The curve-fit derived function describing the relationship between these two parameters was found to be allometric (i.e., power function), with a remarkable R^2 value of 0.88 ($P = 3 \times 10^{-8}$) (Fig. 7A). However, when plotting either the relative ABCG2-IA interaction values (Fig. 7B) or the IA cytotoxicity values (IC_{50}; Fig. 7C) against the calculated log P (ClogP) value of the IAs, no significant correlation was observed.

ABCG2 Confers Differential Resistance to TAs Based on the Presence of a Hydroxyl Group on an R1 Corresponding Position. We have shown that resistance to the lead TA C-1305 in A549/K1.5 cells is mediated by ABCG2 (Bram et al., 2007). Hence, we decided to test our structural observation using this distinct chemical group of nonfluorescent drugs (TA common structure, see Fig. 1) using available OH-bearing and -lacking TAs in a cytotoxicity assay. It is noteworthy that ABCG2-mediated resistance to TAs in A549/K1.5 cells was completely dependent on the presence of a hydroxyl group at the R1 corresponding position. Thus, R1-hydroxyl-containing TAs generated up to 20-fold resistance, whereas hydroxyl-lacking TAs maintained parental cell sensitivity (Table 3).

Mutant Arg482Gly and Arg482Thr ABCG2 Do Not Alter IA Substrate Recognition. Previous reports have established that the Arg482Gly and Arg482Thr ABCG2 mutations resulted in altered substrate specificity and augmented cellular drug resistance (Robey et al., 2003; Shafran et al., 2005; Bram et al., 2006). To determine whether these mutations alter IA substrate specificity and thereby facilitate the efflux of non-ABCG2 substrates of group B IAs, a flow cytometric IA accumulation assay was employed using HEK293 cells stably transfected with wild-type Arg482- as well as mutant Gly482- or T482-ABCG2 (Robey et al., 2003) (Fig. 8). Group A IAs C-1309 and C-1310 were efficiently extruded from both wild-type Arg482 and mutant Gly482- and Thr482-ABCG2-overexpressing cells in a similar manner, but not from untransfected HEK293 cells ($P = 0.0001$ and 0.00015, respectively; Fig. 8). In contrast, Group B IA C-1213 lacking a hydroxyl group remained a nonsubstrate for both wild-type and mutant Gly482/Thr482 ABCG2, with statistically insignificant differences in AF values ($P = 0.22$), compared with nontransfected HEK293 cells (Fig. 8). Likewise, lack of ABCG2-mediated efflux of the long tailed IAs C-1315 and C-2018 was evident in all ABCG2 variants as well ($P = 0.12$ and 0.1, respectively; Fig. 8). Moreover, we have previously shown that TMR efflux is a distinct characteristic of mutant Gly482-/Thr482- but not of wild-type Arg482-ABCG2. Indeed, mutant Gly482- and Thr482-

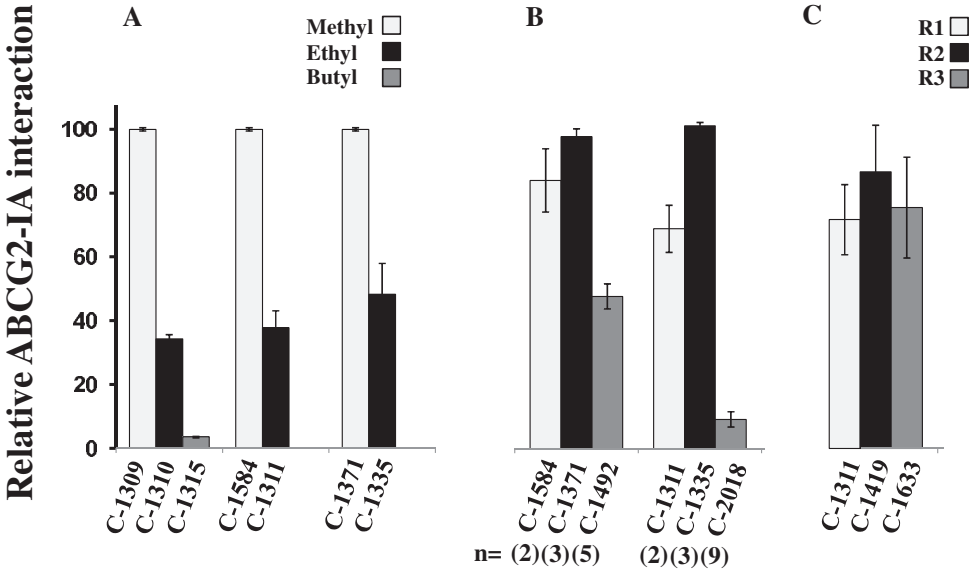

Fig. 6. Structural determinants in the IA side chain affecting interaction of IA with ABCG2. The impact of $R_{a,b}$ size (A), n length (B), and OH position around the outer ring (C) on the interaction of IAs with ABCG2 was determined. IAs were divided into comparable subsets differing only by the single parameter evaluated. Relative interaction of IAs with ABCG2 was assessed using the integrated RF and AF values ± S.E. as specified under *Materials and Methods*.

ABCG2 displayed marked AF toward TMR, whereas wild-type Arg482-ABCG2 overexpressing cells displayed an AF of 1.4, which is comparable with the value (0.8-fold) obtained with untransfected parental HEK293 cells (Fig. 8).

IAs and PhA Do Not Compete on ABCG2-Mediated Efflux. To achieve a better understanding of the difference in the interaction of group A and B IAs with ABCG2, a flow cytometric competition assay was employed using A549/K1.5 cells along with the ABCG2 fluorescent substrate PhA. It is noteworthy that no significant inhibition of PhA efflux was noted when cells were coincubated with a constant concentration of PhA along with group A IAs C-1309 or C-1310 (or C-1492, data not shown) at an IA molar excess of up to 1000-fold (Fig. 9A and B, respectively). Similar results were obtained with the reciprocal experiment in which no increase in the IA (C-1309 and C-1310) accumulation was observed upon coincubation with increasing PhA concentrations (Fig. 9, C and D, respectively). These latter results preclude the possibility that an inefficient competition is due to a marked differential affinity of the different IA substrates for ABCG2. The use of other ABCG2 fluorescent substrates for the competition assay was not possible as a result of either fluorescent spectra overlap or emission quenching (data not shown).

Discussion

In the current article, we have identified key structural determinants of both imidazoacridinones and triazoloacridinones that are crucial for substrate recognition and efflux by ABCG2, as revealed by the following line of evidence:

1. A markedly decreased accumulation of IAs containing a hydroxyl group at one of the R1, R2, or R3 positions was observed in ABCG2-overexpressing A549/K1.5 cells using a flow cytometric assay that takes advantage of the inherent fluorescent properties of IAs. Restoration of cellular accumulation of hydroxyl group-containing IAs was consistently achieved by coincubation with the specific ABCG2 transport inhibitor FTC. In contrast, IAs that lack a hydroxyl group at these positions accumulated to high levels in A549/K1.5 cells, irrespective of ABCG2 expression status.
2. Fluorescence microscopy consistently revealed that ABCG2-overexpressing A549/K1.5 cells failed to stain with hydroxyl group-containing IAs but stained brightly with hydroxyl group-lacking IAs.
3. A549/K1.5 cells displayed marked levels of drug resistance to hydroxyl group-containing IAs but retained parental cell sensitivity to hydroxyl group-lacking IAs. Remarkably, A549/K1.5 cells exhibited marked levels of drug resistance to hydroxyl group-containing TAs but retained wild-type sensitivity to hydroxyl group-lacking TAs.
4. HEK293 cells stably transfected with the wild-type (Arg482) or mutant Gly482/Thr482 ABCG2 cDNAs displayed an excellent extrusion of hydroxyl group containing IAs, whereas FTC fully restored drug accumulation, thereby establishing that both wt and Gly482/Thr482 mutant ABCG2 mediate the efflux of these IAs from ABCG2-overexpressing cells.

The differential interaction of IAs with ABCG2 separated these compounds into two distinct groups [i.e., ABCG2 transport substrates (group A) and nonsubstrates (group B)]. This functional cluster differentiation of IAs was found to depend on two basic IA structural features: 1) the presence or absence of a hydroxyl group at one of the R1, R2, or R3 positions located around the outer proximal IA ring and 2) the linear

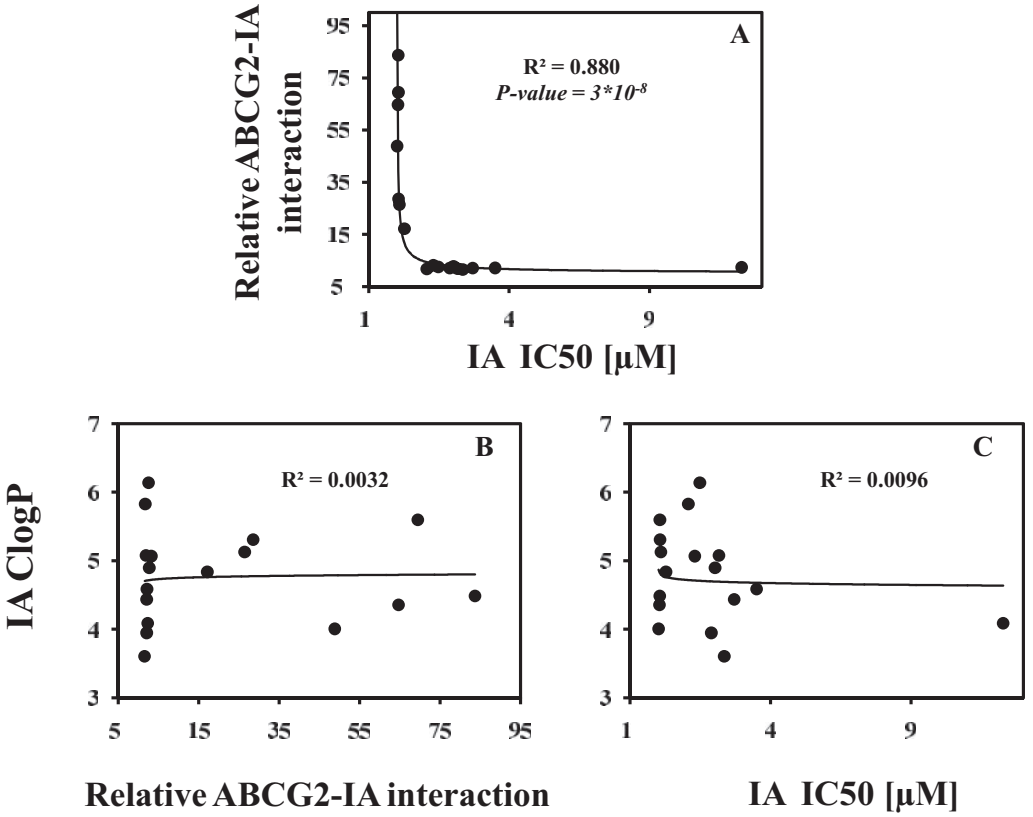

Fig. 7. The interaction of IAs with ABCG2 correlates with the cytotoxic capacity of IAs. The integrated relative IA-ABCG2 interaction values of all short tail IAs (17 IAs in which $n \leq 3$ and $R_{a,b} \leq$ ethyl) were plotted against their IC_{50} values in ABCG2-lacking drug sensitive parental A549 cells (A) or against their ClogP values (B). Moreover, the IC_{50} values of IAs were plotted against their ClogP values (C). Regression curves and R^2 values for these data sets are presented; short-tail IAs used: C-1584, C-1371, C-1309, C-1310, C-1336, C-1335, C-1311, C-1379, C-1375, C-1558, C-1212, C-1554, C-1330, C-1176, C-1415, C-1503, and C-1213, consisting of all short side-chain IAs differing solely by the presence or absence of the proximal ring OH− group.

and/or branched length of the IA distal side chain tail. The most prominent feature of IAs from group A of ABCG2 transport substrates was the presence of a hydroxyl group at one of the R1, R2, or R3 positions. These positions are located at the outskirts of the IA molecule and are readily accessible to direct interaction with their environment, most likely as hydrogen bond donors. Moreover, we found that the presence of a corresponding R1 position hydroxyl is necessary to facilitate ABCG2-mediated drug resistance also toward the distinct pharmacological group of TAs. In accord, a recent study on the nature of ABCG2 interaction with camptothecin analogs has revealed a similar dependence on the presence of hydroxyl or amine groups on the outer ring of their common camptothecin structure, possibly facilitating hydrogen bond formation, essential for substrate recognition and efflux via ABCG2; these camptothecin positions seem to be analogous to the present R1, R2, or R3 positions of IAs (Yoshikawa et al., 2004). Several subsequent publications on ABCG2-dependent resistance to novel camptothecin analogs have also obeyed this general hydrogen bond rule (Rajendra et al., 2003; Bates et al., 2004; Takagi et al., 2007). Hence, these cumulative results emphasize the robustness of basic structural features of ABCG2 efflux substrates from diverse groups of polyaromatic cytotoxic agents. Furthermore, a close inspection of established ABCG2 substrates, such as SN-38, mitoxantrone, and methotrexate reveals a distinct candidate for putative hydrogen-bond formation at a corresponding position of their polycyclic ring (Fig. 1, see groups in red). Accordingly, nonsubstrates of ABCG2 with similar polycyclic structure lack the corresponding group, presumably facilitating hydrogen-bond formation (Fig. 1). An important functional implication of the essential role that putative hydrogen bond formation plays in the interaction of ABCG2 with its substrates in the extrusion of endo- and xenobiotics relates to the transport capacity of ABCG2 and other MDR efflux transporters. MDR transporters of the ABC superfamily, including ABCB1, ABCC1, and ABCG2, are relatively low-affinity yet high-capacity drug efflux transporters (Borgnia et al., 1996; Eytan et al., 1996; Assaraf, 2006; Assaraf, 2007). Our current findings of the putative hydrogen bond formation of IA substrates with ABCG2 are in agreement with the thorough analysis of Omote and Al-Shawi (Al-Shawi et al., 2003) who found a tight correlation between the relatively weak drug-transporter hydrogen bond formation and the high capacity of drug extrusion by ABCB1.

TABLE 3

Summary of growth inhibition studies on parental A549 and ABCG2 expressing A549/K1.5 cells upon 120 h exposure to the various TAs

IC_{50} was evaluated using the MTT assay. Two-dimensional structural comparison of the various TAs is shown in the right column. TA common structure is presented in Fig. 1.

Drug	IC_{50}		RF	TA Structure		
	A549	A549/K1.5		R1	$R_{a,b}$	*n*
	μM					
Group A						
C-1305	0.16 ± 0.12	3.02 ± 0.42	20	OH	Me	3
C-2007	1.66 ± 0.22	15.6 ± 0.82	9.1	OH	Me	4
C-1293	0.038 ± 0.03	0.30 ± 0.08	7.9	OH	Et	3
Group B						
C-1234	2.27 ± 0.12	1.83 ± 0.32	0.8	H	Me	3
C-1296	0.85 ± 0.05	1.57 ± 0.15	1.8	Me	Me	2
C-1299	0.66 ± 0.15	0.36 ± 0.12	0.5	OMe	Me	3

The bioactivation, metabolism, and/or detoxification of natural and synthetic polyaromatic molecules, including anthracene derivatives and benzopyrene, are achieved via hydroxylation at sites analogous to the R1, R2, or R3 positions of IAs. Most of these compounds are considered genotoxic, mutagenic, and carcinogenic agents and are ubiquitously found in plants and overcooked food. Although modern human dietary intake of these phytotoxins seems to be nonhazardous (Mueller et al., 1999), this may very well not be the case for our herbivorous predecessors. Accordingly, IA cytotoxicity seemed to depend on the presence of a hydroxyl group at position R1. IAs possessing this feature maintained up to two orders of magnitude increased cytotoxicity toward ABCG2-lacking A549 lung cancer cells. This observation was corroborated in previous reports on IA cytotoxicity using different model cell lines (Cholody et al., 1990a; Burger et al., 1996; Dziegielewski et al., 2002). Although this observation may hamper the ability to rationally design highly toxic IAs also able to circumvent ABCG2-mediated MDR, it bears profound implications for the evolution of ABCG2 from ancestral bacterial genes encoding cytotoxic drug efflux transporters. The remarkable correlation between ABCG2 substrate recognition and IA toxicity through the same IA structural determinants may suggest a coevolutionary process of endo- and xenobiotic efflux pumps. Therefore, the exact same structural determinants mediat-

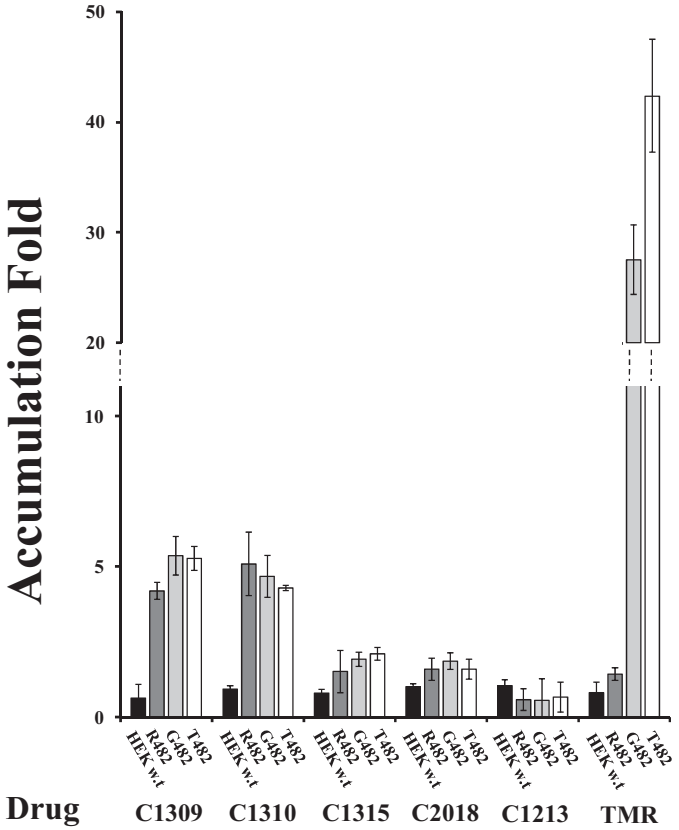

Fig. 8. IA accumulation in HEK293 transfectant cells stably overexpressing wild-type Arg482 ABCG2 or mutant R482G/T ABCG2 in the presence or absence of fumitremorgin C. Cells were suspended in medium buffered with 20 mM HEPES, pH 7.3, and incubated either with 1 μM concentrations of selected group A and B IAs or with 100 nM tetramethylrosamine at 37°C for 1 h in the presence and absence of 5 μM FTC. Results represent the mean FTC-inducible AF value of each IA in wild-type and mutant ABCG2-overexpressing cells. Mean values ± S.D. were obtained from at least three independent experiments.

ing IA toxicity and possibly the bioactivity of other polyaromatic molecules are the target of interest for ABCG2 substrate recognition and consequent drug efflux. Further confirmation of this possible coevolution may be supported by a recent study demonstrating an endogenous cellular response pathway to ABCG2 genotoxic substrates, resulting in the functional up-regulation of ABCG2 in the colon cancer Caco2 cell line exposed to various phytochemicals and polyaromatic hydrocarbons (e.g., benzopyrene), presumably via the aryl hydrocarbon receptor pathway (Ebert et al., 2005, 2007; Wang, 2007).

Whereas the presence or absence of the facilitating hydroxyl group has an all-or-none impact on whether ABCG2 interacts with IAs, the inhibitory effect that the length of the IA tail has on the ability of ABCG2 to recognize these compounds as transport substrates seems to be gradual. Our findings suggest that elongation of the aliphatic side chain tail (n) produces a relatively moderate interference in the interaction of IAs with ABCG2, which becomes significant only when IAs contain relatively longer side-chain tails ($n \geq 5$). In contrast, modest elongations of the branched $R_{a,b}$ tail group have a marked impact on the ability of ABCG2 to recognize and extrude IAs; this is possibly due to the branched nature of the $R_{a,b}$ group, presumably leading to the simultaneous elongation of the dual tails, thereby markedly contributing to increased bulk of IAs. Hence, elongation of the IA tail may disrupt the optimal bulk fit of IAs in the putative ABCG2 pharmacophore, thereby precluding drug recognition and subsequent efflux. This negative side-chain effect on ABCG2 efflux activity may resemble the negative impact of folate and anti-folate poly-γ-glutamylation via folylpolyglutamate synthetase activity on ABCG2-mediated efflux (Shafran et al., 2005), demonstrating a general constraint on ABCG2 substrate size and bulk. This presumption is of interest because of the broad spectrum of large substrates that are efficiently extruded by ABCG2 including the chlorophyll derivative PhA and the hemoglobin component porphyrin (Jonker et al., 2002, 2007), both of which seem to exceed the typical size of IAs. The lack of significant ABCG2-mediated efflux competition between group A IAs and PhA observed in our current study supports a recent report suggesting multiple allosteric substrate-binding sites for ABCG2, based upon differential substrate interaction kinetics with this transporter (Clark et al., 2006). This study was recently corroborated by the finding of an allosteric functional steroid binding element in ABCG2's transmembrane domain, thereby being distinct from the drug binding site of the transporter (Velamakanni et al., 2008).

One of the major aims of the current research is to develop novel strategies that overcome drug resistance phenomena,

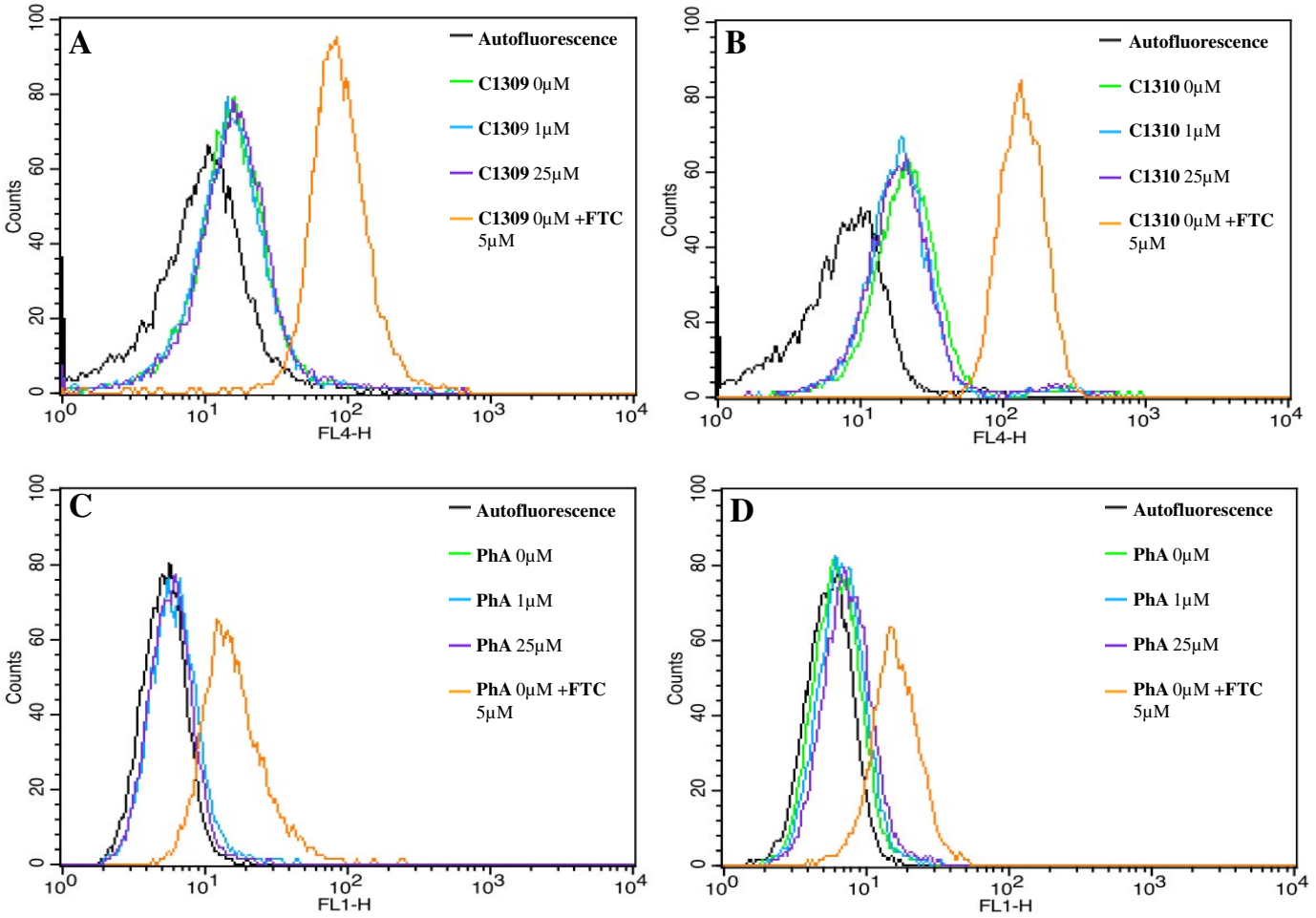

Fig. 9. Intracellular accumulation of representative group A IAs or PhA in the presence or absence of reciprocal PhA or group A IA competition. Cells were suspended in medium buffered with 20 mM HEPES, pH 7.3, and incubated at 37°C for 1 h either with 25 nM PhA (A or B) or selected group A IAs C-1309 (C) and C-1310 (D). PhA-containing samples were coincubated either with 0, 1, and 25 μM C-1309 or 5 μM FTC (A) or with corresponding C-1310 concentrations (B). Likewise, IA-containing samples (C and D) were coincubated with increasing PhA concentrations or 5 μM FTC.

particularly those that are associated with ABC transporter-based MDR. In the present study, we found that A549/K1.5 cells that display a marked ABCG2-dependent resistance to group A IAs were up to 5-fold more sensitive to hydroxyl group-lacking IAs, including C-1266. Hence, this observation has important implications for further development of novel cytotoxic agents that not only fail to be recognized by ABCG2 but that can exert a specific increased cytotoxicity to ABCG2-overexpressing cells via some as-yet unknown biochemical alteration, thereby rendering MDR cells highly susceptible to these antitumor agents. In this respect, further studies are warranted that, on the one hand, use C-1266 as a lead compound upon a high-throughput screening of a large library of small molecules aimed at identification of novel compounds that achieve an augmented hypersensitization effect in ABCG2-overexpressing cells. On the other hand, the biochemical basis underlying this marked and selective hypersensitivity of ABCG2-dependent MDR cells to certain cytotoxic agents requires detailed studies that may pinpoint the underlying molecular mechanism of hypersensitivity. Clearly, such studies have major implications for the overcoming of clinical chemoresistance based upon frequently emerging ABCG2-dependent MDR phenomena.

Acknowledgments

This article is dedicated to the late Amiel Bney-Moshe.

References

Al-Shawi MK, Polar MK, Omote H, and Figler RA (2003) Transition state analysis of the coupling of drug transport to ATP hydrolysis by P-glycoprotein. *J Biol Chem* **278:**52629–52640.

Alami N, Paterson J, Belanger S, Juste S, Grieshaber CK, and Leyland-Jones B (2007) Comparative cytotoxicity of C-1311 in colon cancer in vitro and in vivo using the hollow fiber assay. *J Chemother* **19:**546–553.

Assaraf YG (2006) The role of multidrug resistance efflux transporters in antifolate resistance and folate homeostasis. *Drug Resist Updat* **9:**227–246.

Assaraf YG (2007) Molecular basis of antifolate resistance. *Cancer Metastasis Rev* **26:**153–181.

Bates SE, Medina-Pérez WY, Kohlhagen G, Antony S, Nadjem T, Robey RW, and Pommier Y (2004) ABCG2 mediates differential resistance to SN-38 (7-ethyl-10-hydroxycamptothecin) and homocamptothecins. *J Pharmacol Exp Ther* **310:**836–842.

Belmont P, Bosson J, Godet T, and Tiano M (2007) Acridine and acridone derivatives, anticancer properties and synthetic methods: where are we now? *Anticancer Agents Med Chem* **7:**139–169.

Borgnia MJ, Eytan GD, and Assaraf YG (1996) Competition of hydrophobic peptides, cytotoxic drugs, and chemosensitizers on a common P-glycoprotein pharmacophore as revealed by its ATPase activity. *J Biol Chem* **271:**3163–3171.

Borst P and Elferink RO (2002) Mammalian ABC transporters in health and disease. *Annu Rev Biochem* **71:**537–592.

Bram E, Ifergan I, Shafran A, Berman B, Jansen G, and Assaraf YG (2006) Mutant Gly482 and Thr482 ABCG2 mediate high-level resistance to lipophilic antifolates. *Cancer Chemother Pharmacol* **58:**826–834.

Bram EE, Ifergan I, Grimberg M, Lemke K, Skladanowski A, and Assaraf YG (2007) C421 allele-specific ABCG2 gene amplification confers resistance to the antitumor triazoloacridone C-1305 in human lung cancer cells. *Biochem Pharmacol* **74:**41–53.

Burger AM, Double JA, Konopa J, and Bibby MC (1996) Preclinical evaluation of novel imidazoacridinone derivatives with potent activity against experimental colorectal cancer. *Br J Cancer* **74:**1369–1374.

Cholody WM, Martelli S, and Konopa J (1990a) 8-Substituted 5-[(aminoalkyl)amino]-6H-v-triazolo[4,5,1-de]acridin-6-ones as potential antineoplastic agents. Synthesis and biological activity. *J Med Chem* **33:**2852–2856.

Cholody WM, Martelli S, Paradziej-Lukowicz J, and Konopa J (1990b) 5-[(Aminoalkyl)amino]imidazo[4,5,1-de]acridin-6-ones as a novel class of antineoplastic agents. Synthesis and biological activity. *J Med Chem* **33:**49–52.

Clark R, Kerr ID, and Callaghan R (2006) Multiple drugbinding sites on the R482G isoform of the ABCG2 transporter. *Br J Pharmacol* **149:**506–515.

Deeley RG, Westlake C, and Cole SP (2006) Transmembrane transport of endo- and xenobiotics by mammalian ATP-binding cassette multidrug resistance proteins. *Physiol Rev* **86:**849–899.

Doyle LA and Ross DD (2003) Multidrug resistance mediated by the breast cancer resistance protein BCRP (ABCG2). *Oncogene* **22:**7340–7358.

Dziegielewski J, Slusarski B, Konitz A, Skladanowski A, and Konopa J (2002) Intercalation of imidazoacridinones to DNA and its relevance to cytotoxic and antitumor activity. *Biochem Pharmacol* **63:**1653–1662.

Ebert B, Seidel A, and Lampen A (2005) Identification of BCRP as transporter of benzo[a]pyrene conjugates metabolically formed in Caco-2 cells and its induction by Ah-receptor agonists. *Carcinogenesis* **26:**1754–1763.

Ebert B, Seidel A, and Lampen A (2007) Phytochemicals induce breast cancer resistance protein in Caco-2 cells and enhance the transport of benzo[a]pyrene-3-sulfate. *Toxicol Sci* **96:**227–236.

Eytan GD, Regev R, and Assaraf YG (1996) Functional reconstitution of P-glycoprotein reveals an apparent near stoichiometric drug transport to ATP hydrolysis. *J Biol Chem* **271:**3172–3178.

Goodman K, Duncan K, Locniskar A and Ajami A (2008) SymadexTM, a FLT3 kinase inhibitor, is metabolized by aldehyde oxidase. *FASEB J* **22:**920.5.

Hyzy M, Bozko P, Konopa J, and Skladanowski A (2005) Antitumour imidazoacridone C-1311 induces cell death by mitotic catastrophe in human colon carcinoma cells. *Biochem Pharmacol* **69:**801–809.

Jonker JW, Buitelaar M, Wagenaar E, Van Der Valk MA, Scheffer GL, Scheper RJ, Plosch T, Kuipers F, Elferink RP, Rosing H, et al. (2002) The breast cancer resistance protein protects against a major chlorophyll-derived dietary phototoxin and protoporphyria. *Proc Natl Acad Sci U S A* **99:**15649–15654.

Jonker JW, Musters S, Vlaming ML, Plösch T, Gooijert KE, Hillebrand MJ, Rosing H, Beijnen JH, Verkade HJ, and Schinkel AH (2007) Breast cancer resistance protein (Bcrp1/Abcg2) is expressed in the harderian gland and mediates transport of conjugated protoporphyrin IX. *Am J Physiol Cell Physiol* **292:**C2204–C2212.

Kusnierczyk H, Cholody WM, Paradziej-Lukowicz J, Radzikowski C and Konopa J (1994) Experimental antitumor activity and toxicity of the selected triazolo- and imidazoacridinones. *Arch Immunol Ther Exp* (*Warsz*) **42:**415–423.

Modok S, Mellor HR, and Callaghan R (2006) Modulation of multidrug resistance efflux pump activity to overcome chemoresistance in cancer. *Curr Opin Pharmacol* **6:**350–354.

Mueller SO, Schmitt M, Dekant W, Stopper H, Schlatter J, Schreier P, and Lutz WK (1999) Occurrence of emodin, chrysophanol and physcion in vegetables, herbs and liquors. Genotoxicity and anti-genotoxicity of the anthraquinones and of the whole plants. *Food Chem Toxicol* **37:**481–491.

Nakanishi T, Karp JE, Tan M, Doyle LA, Peters T, Yang W, Wei D, and Ross DD (2003) Quantitative analysis of breast cancer resistance protein and cellular resistance to flavopiridol in acute leukemia patients. *Clin Cancer Res* **9:**3320–3328.

Poindessous V, Koeppel F, Raymond E, Comisso M, Waters SJ, and Larsen AK (2003) Marked activity of irofulven toward human carcinoma cells: comparison with cisplatin and ecteinascidin. *Clin Cancer Res* **9:**2817–2825.

Polgar O, Robey RW, and Bates SE (2008) ABCG2: structure, function and role in drug response. *Expert Opin Drug Metab Toxicol* **4:**1–15.

Rabindran SK, Ross DD, Doyle LA, Yang W, and Greenberger LM (2000) Fumitremorgin C reverses multidrug resistance in cells transfected with the breast cancer resistance protein. *Cancer Res* **60:**47–50.

Rajendra R, Gounder MK, Saleem A, Schellens JH, Ross DD, Bates SE, Sinko P, and Rubin EH (2003) Differential effects of the breast cancer resistance protein on the cellular accumulation and cytotoxicity of 9-aminocamptothecin and 9-nitrocamptothecin. *Cancer Res* **63:**3228–3233.

Robey RW, Honjo Y, Morisaki K, Nadjem TA, Runge S, Risbood M, Poruchynsky MS, and Bates SE (2003) Mutations at amino-acid 482 in the ABCG2 gene affect substrate and antagonist specificity. *Br J Cancer* **89:**1971–1978.

Ross DD, Karp JE, Chen TT, and Doyle LA (2000) Expression of breast cancer resistance protein in blast cells from patients with acute leukemia. *Blood* **96:**365–368.

Sarkadi B, Homolya L, Szakács G, and Váradi A (2006) Human multidrug resistance ABCB and ABCG transporters: participation in a chemoimmunity defense system. *Physiol Rev* **86:**1179–1236.

Shafran A, Ifergan I, Bram E, Jansen G, Kathmann I, Peters GJ, Robey RW, Bates SE, and Assaraf YG (2005) ABCG2 harboring the Gly482 mutation confers high-level resistance to various hydrophilic antifolates. *Cancer Res* **65:**8414–8422.

Sharom FJ (2008) ABC multidrug transporters: structure, function and role in chemoresistance. *Pharmacogenomics* **9:**105–127.

Stam RW, van den Heuvel-Eibrink MM, den Boer ML, Ebus ME, Janka-Schaub GE, Allen JD, and Pieters R (2004) Multidrug resistance genes in infant acute lymphoblastic leukemia: Ara-C is not a substrate for the breast cancer resistance protein. *Leukemia* **18:**78–83.

Steinbach D, Sell W, Voigt A, Hermann J, Zintl F, and Sauerbrey A (2002) BCRP gene expression is associated with a poor response to remission induction therapy in childhood acute myeloid leukemia. *Leukemia* **16:**1443–1447.

Takagi K, Dexheimer TS, Redon C, Sordet O, Agama K, Lavielle G, Pierré A, Bates SE, and Pommier Y (2007) Novel E-ring camptothecin keto analogues (S38809 and S39625) are stable, potent, and selective topoisomerase I inhibitors without being substrates of drug efflux transporters. *Mol Cancer Ther* **6:**3229–3238.

Topcu Z (2001) DNA topoisomerases as targets for anticancer drugs. *J Clin Pharm Ther* **26:**405–416.

Turner JG, Gump JL, Zhang C, Cook JM, Marchion D, Hazlehurst L, Munster P, Schell MJ, Dalton WS, and Sullivan DM (2006) ABCG2 expression, function, and promoter methylation in human multiple myeloma. *Blood* **108:**3881–3889.

van den Heuvel-Eibrink MM, Wiemer EA, Prins A, Meijerink JP, Vossebeld PJ, van der Holt B, Pieters R, and Sonneveld P (2002) Increased expression of the breast cancer resistance protein (BCRP) in relapsed or refractory acute myeloid leukemia (AML). *Leukemia* **16:**833–839.

Velamakanni S, Janvilisri T, Shahi S, and van Veen HW (2008) A functional steroid-binding element in an ATP-binding cassette multidrug transporter. *Mol Pharmacol* **73:**12–17.

Wang M (2007) Extending the good diet, good health paradigm: modulation of breast cancer resistance protein (BCRP) by flavonoids. *Toxicol Sci* **96:**203–205.

Yoshikawa M, Ikegami Y, Hayasaka S, Ishii K, Ito A, Sano K, Suzuki T, Togawa T, Yoshida H, Soda H, et al. (2004) Novel camptothecin analogues that circumvent ABCG2-associated drug resistance in human tumor cells. *Int J Cancer* **110:**921–927.

Address correspondence to: Yehuda G. Assaraf, The Fred Wyszkowski Cancer Research Laboratory, Department of Biology, Technion-Israel Institute of Technology, Haifa 32000, Israel. E-mail: assaraf@tx.technion.ac.il